

Time Reversed Ultra-Wideband (UWB) Multiple-Input Multiple-Output (MIMO) Based on Measured Spatial Channels

Chenming Zhou

Department of Electrical and Computer Engineering

Carnegie Mellon University

Pittsburgh, PA 15213

Email: czhou@cmu.edu

Nan Guo, and Robert C. Qiu (Contact Author)

Department of Electrical and Computer Engineering

Center for Manufacturing Research

Tennessee Technological University

Cookeville, TN 38505

Email: {[nguo](mailto:nguo@tntech.edu), [rqi](mailto:rqi@tntech.edu)} @tntech.edu

Abstract

UWB technology is envisioned for future wireless high data rate transmission. A UWB system with multiple antennas takes advantage of the rich scattering environment to increase the data rate. On the other hand, given rich multipath, Time Reversal (TR) uses scatterers to create space and time focalization at a target point by coherent addition of all scattered contributions at that point. This paper analyzes the performance of an impulse TR-MIMO-UWB system with a simple one-correlator receiver. The performance analyses are based on UWB spatial channels measured in an office environment.

Index Terms

Impulse Multiple-Input Multiple-Output (MIMO), time reversal, Ultra-wideband (UWB), rich multipath, spatial focusing, inter-symbol-interference (ISI)

I. INTRODUCTION

Ultra-wideband (UWB) transmission has recently emerged as a potential candidate for future high data rate applications [1] - [7]. Impulsive transmission with short pulse duration makes the multipath components resolvable, which in turn leads to immunity to the multipath fading. On the other hand, however, capture of multipath energy distributed in dense multipath components becomes a challenge. Time Reversal (TR) signal processing, a signal processing technique popular in acoustics [8], has been applied to electromagnetics [9] - [21] recently. A tutorial of time reversal and an extensive review of literature for UWB communications is given in [14]. An attractive aspect of TR signal processing is the fact that it makes use of multipath propagation. UWB impulsive radio is extremely interesting in this context, since hundreds or thousands of paths are available, see e.g. [17] [19].

Given a specific time and location, TR precoding has been mathematically proved to be the optimum in the sense that it maximizes the amplitude of the field at that time and location [22]. It is then called spatio-temporal matched filter [23], because it is analogous to a matched filter both in time and space. It is also called transmit matched filter since the matched filter is put at the transmitter side. However, TR alone may not effectively reduce the channel delay spread, considering the fact it maximizes the peak amplitude but does not impose any constraint at its sidelobe level. As shown in [21], multiple antennas at the transmitter (MISO-TR) are, then, required to suppress the inter symbol interference (ISI). The MISO-TR scheme also achieves array gain with a factor of M (antenna number), by automatically aligning the arrival peak [24]. MISO-TR has been investigated extensively in the past years (e.g., [25] and [26]), and a natural extension is to exploit the scenario of Multiple-Input and Multiple-Output (MIMO) for TR signaling.

MIMO technique uses multiple antennas at both ends of the wireless link and is believed to be the most promising approach to effectively use the transmission spectrum and power. This technology has been extensively studied recently [27], [28]. It has been shown that the channel capacity for a MIMO system is increased as the number of antennas increases. MIMO is mostly used in conjunction with Orthogonal Frequency-Dimension Modulation (OFDM), a modulation technology that is part of the *IEEE 802.16* standard and will also be part of the *IEEE 802.11n* high-throughput standard, due to its potentially high data rate capability. In addition to the

benefit from flat fading, MIMO also benefits from the rich scattering of the channel. To employ multiple antennas and space time signal processing in a UWB system has been an interesting topic [29]–[31].

MIMO-UWB is a concept that can be implemented in several alternative ways; in addition to the OFDM MIMO mentioned above, another way is based on a scheme using impulse radio to transmit pulses in one or multiple frequency bands, such as the multiband UWB (MB-UWB) solution [32]. Here, we propose to use TR precoding combined with MIMO [33], called impulse MIMO-TR. Note that we are interested in the limits of UWB signals, i.e. pulses with ultra-short duration and extremely wide bandwidth. The proposed MIMO-TR aims to implement MIMO directly in time domain, and hence is believed to be a simpler scheme than its frequency domain counterpart. However, most research on UWB-MIMO is carried out in the frequency domain, very few time domain UWB MIMO results are reported. [34] proposed to use Maximal Ratio Combining (MRC) RAKE combining to accomplish the temporal alignment of received pulses, which causes huge complexity at the receiver. However, pulses are automatically aligned by using of TR precoding at the cost of increased transmitter complexity. It is shown in [35] that TR precoding can achieve the same error performance as the MRC combining scheme.

Separating the data streams at the receiver is challenging for parallel data transmission. For the traditional narrow band MIMO, singular-value decomposition (SVD) is usually applied to decompose the channel into several independent subchannels. For multi-tone UWB signals with Giga Hertz bandwidth, however, applying SVD to each frequency tone significantly increases the system complexity. In [36], a zero-forcing scheme is proposed to separate N parallel transmitted data streams for each resolvable multipath component. In this paper, considering the good spatial-temporal focusing characteristics provided by TR, we will show that TR precoding can also decompose the channel, with reasonable complexity. The primary motivation of this research is to investigate a system structure that has a good trade-off between complexity and performance. MIMO-TR is such a structure.

Although MIMO-TR can achieve high data rate by parallel data transmission, the applications of MIMO-TR are not limited to support of high data rate. With a beamforming approach, where all the transmitter antenna elements transmit the same information bit, high signal-to-noise ratio (SNR) can be obtained at the receiver, and hence the transmission distance can be greatly extended, depending on the number of antennas employed in the array. It is shown in this

paper that given the same transmission power, the peak SNR at the receiver grows linearly with the numbers M (number of transmitter antenna elements) and N (number of receiver antenna elements).

The philosophy behind TR is the so called transmit centric processing, i.e., processing the signal at the transmitter side before transmission to combat the deteriorating effects of the channel. The motivation is from the fact that the power and computation resources are generally more readily available at the transmitter side. The main advantage of transmit centric processing is the possibility to simplify the receivers, which is desirable in the case of one central node serving for many distributed sensor nodes.

Due to the favorable spatial-temporally focusing of the MIMO-TR technique, the energy of a receive signal tends to focus into a geometric spot and into a time instant. We propose to use a simple coherent receiver with one correlator to capture the peak energy, and ignore the rest of the energy as interference. By doing this, the receiver complexity can be greatly reduced, since there are no channel estimation and equalization in the receiver. However, as we will show later, the performance of such a simple receiver can still achieve the Additive White Gaussian Noise (AWGN) bound under ideal conditions that all the multipath components are resolvable and there is no ISI in the system, given the same transmitted power. An energy gain of $10\log_{10}(MN)$ dB can be achieved by using a MIMO system with M antennas at the transmitter and N antennas at the receiver. We also investigate the performance based on the bit energy at the receiver. We compare the performances for different scenarios (MIMO, MISO, and SISO), considering one-correlator receiver.

In practice, when a pulse is short and the data rate is low, the above conditions (resolvable multipath and no ISI) tend to be satisfied. However, for the case of high data rate and relatively wide pulses, the conditions will not hold any more. The performance of such a practical system is investigated through Monte Carlo simulation. There are no data (on the channel model of multiple antennas) that meet the need of this research for spatial-temporal focusing; we have conducted a series of channel measurements in an office environment. The measurements are performed in the time domain, and the CLEAN algorithm [48], [49] is employed to extract the channel impulse response (CIR) from the measured data.

Time reversal with multi-user UWB communications has been studied by some other researchers (e.g., in [44]–[47]) and the single user scenario has been considered in this paper.

The structure of this paper is as follows: The principle of time reversal signal processing and its sub-optimum receiver—one-correlator receiver are introduced in Section II. The system performance analysis for single antenna at both ends is given in Section III. Then the performance analysis is extended to multiple antennas scenarios, in Sections IV and V. The experimental description regarding the channel measurements are shown in Section VI. Numerical results based on the measured spatial channels are given in Section VII. Finally, we conclude the paper in Section VIII.

II. PRINCIPLE OF TIME REVERSAL SIGNAL PROCESSING

A. *Spatial-Temporal Focusing Through Time Reversal: Exploitation of Space-Time Symmetry*

Time reversal cannot be understood, at first thought, as a simple scheme: moving the matched filter to the transmitter side as a time reversal filter. There is deep physics in the scheme to exploit the spatial-temporal focusing—unique to impulsive UWB signals. The physical foundation of time reversal is the space-time symmetry, e.g., in general relativity. To avoid digressing too far, we only outline—trying our best to use communications engineers language—the physical mechanism behind the time reversal scheme, since a lot of confusion has been caused in the literature, due to the lack of understanding of this mechanism. The main motivation of this summary of known physical results is to strike the point that the space-time symmetry cannot be taken for granted: it must be first examined, before its wide use. So far, this symmetry principle is established only for some very simplistic physical regions. The experimental approach must be used for realistic system settings, to empirically support this claim. The state-of-the-art status of theoretical justification for the principle of space-time symmetry in a macroscopic phenomenon level is far from satisfactory, especially for realistic UWB communications applications.

It is well known that space-time symmetry is universally true in physics. Radio waves follow the law of electromagnetics: the knowledge of symmetry (reciprocity) properties of a field frequently facilitates the determination of explicit field solutions [38]. For this purpose, one considers certain auxiliary or adjoint problems, related to the original field problem, in such a way as to reveal the space-time symmetry of the original field.

If the field problems are phrased in terms of Green's functions—or channel impulse response (CIR) in linear system terms—which describe the field response to a “point-source excitation,” the desired properties appear most succinctly as symmetries in these Green's functions. A rigorous

derivation of these symmetries in inhomogeneous, lossy media, which is the case of UWB communications, is too difficult. Rather, some insight can be gained using simplified physical model. Experimental results are used to approximately establish the symmetries, for realistic environments, e.g., indoors¹, and intra-vehicle environments [15].

For homogeneous media, or vacuum, the symmetries are analytically established in (Ch.1, [38]). If field symmetries exist, the properties of the electromagnetic Green's functions (thus CIRs) can be inferred prior to their explicit determination. In an *unbounded, homogeneous, stationary* region, the field equations are invariant under arbitrary linear space-time displacements, i.e., the solutions are functions of the differences $\mathbf{r} - \mathbf{r}'$ and $t - t'$, where a pair of any space-time points (\mathbf{r}, t) and (\mathbf{r}', t') is considered. Mathematically, the Green's function has the symmetric form of

$$g(\mathbf{r}, \mathbf{r}'; t, t') = g(\mathbf{r} - \mathbf{r}'; t - t') \quad (1)$$

If we exchange the space-time point (\mathbf{r}, t) with (\mathbf{r}', t') , implying $(\mathbf{r}' - \mathbf{r}; t' - t)$, the Green's function is invariant. In other words, when the spatial locations of two antennas are switched, implying $\mathbf{r}' - \mathbf{r}$, and the time is reversed, implying $t' - t$, the resultant Green's function is identical to the original one. Eq. (1) is exactly the foundation of the so-called time reversal scheme, requiring both time reversal of the CIR measured in one direction and exchange of two spatial locations of the involved antenna pair.

Eq. (1) is valid for the unbounded, homogeneous, stationary region with point-source excitation (ideal impulsive antenna). For a general medium (channel), the adjoint-field problem needs to be solved, using a temporal and spatial reflection transformation [38]. As pointed out above, for the general lossy, bounded, inhomogeneous and moving region with non-point-source excitation (realistic UWB antennas), the adjoint-field problem is open. Some simple physical media are solved, including [38]: (1) free space (unbounded and homogeneous) with point-source excitation; (2) homogeneous medium with point-source excitation for both bounded region; (3) free space with an electrical dipole current excitation; (4) free space with planar stratified scattering structures with Hertz potential excitation; (5) bounded, cylindrical regions (a uniform waveguide

¹To the best knowledge of us, this is the first reported experimental result, in the field of UWB communications, regarding the channel's space-time symmetry.

of arbitrary cross section transverse to the guide axis, and bounded by perfectly conducting walls).

B. Time Reversal: Spatial-Temporal Matched Filter at Transmitter

Consider a communication system illustrated in Fig. 1(a). Here, $p(t)$ is the transmitted pulse waveform, and $h(t)$ denotes the impulse response of the multipath channel. The received signal before $c_1(t)$ can be written as $r(t) = p(t) * h(t) + n(t) = y(t) + n(t)$, where $n(t)$ is AWGN with a two-sided power spectral density of $N_0/2$, and $y(t) = p(t) * h(t)$. Given $r(t)$, a matched filter $y(-t)$, matched to $y(t)$, provides the maximum signal-to-noise power ratio at its output. The matched filter here can be virtually decomposed into two filters, with the first filter matched to the CIR $h(t)$ and the second one matched to the pulse waveform $p(t)$. As shown in Fig. 1(a), this decomposition can be done by setting $c_1(t) = h(-t)$ and $c_2(t) = p(-t)$.

We shall now consider what happens if we move the receiver front-end matched filter $c_1(t)$ to the transmitter, but still keep the filter $c_2(t)$ at the receiver, as depicted in Fig. 1(b). This leads to a time reversal system that is of interest in this paper. Note that this operation actually makes the receiver sub-optimum, as will be shown later. However, by doing this, we simplify the receiver structure and make more effective use of the transmitter energy by concentrating it in the favorable frequency regions.

We still let $c_2(t) = p(-t)$ and wish to find the optimum $c_1(t)$ such that it maximizes the SNR at the output of $c_2(t)$,

$$SNR_1 = \frac{2 \left| \int_{-\infty}^{+\infty} P(f) P^*(f) C_1(f) H(f) df \right|^2}{N_0 \int_{-\infty}^{+\infty} |P(f)|^2 df} \quad (2)$$

under the constraint of fixed transmitted power

$$P_1 = \int_{-\infty}^{+\infty} |P(f) C_1(f)|^2 df. \quad (3)$$

Here $P(f)$, $H(f)$, $C_1(f)$ and $C_2(f)$ are the Fourier transforms of $p(t)$, $h(t)$, $c_1(t)$ and $c_2(t)$, respectively. Note that the denominator of (2) does not depend on $C_1(f)$. To maximize (2),

equivalently, we need to maximize the ratio

$$\rho = \frac{\left| \int_{-\infty}^{+\infty} |P(f)|^2 C_1(f) H(f) df \right|^2}{\int_{-\infty}^{+\infty} |P(f) C_1(f)|^2 df}. \quad (4)$$

According to Schwartz inequality, we have

$$\left| \int_{-\infty}^{+\infty} P(f) C_1(f) H(f) P^*(f) df \right|^2 \leq \int_{-\infty}^{+\infty} |P(f) C_1(f)|^2 df \bullet \int_{-\infty}^{+\infty} |P^*(f) H(f)|^2 df. \quad (5)$$

substitution of (5) into (4) yields

$$\rho \leq \int_{-\infty}^{+\infty} |P^*(f) H(f)|^2 df. \quad (6)$$

with equality holding only when $C_1(f) = \lambda_1 H^*(f)$, or in time domain, $c_1(t) = \lambda_1 h(-t)$, where λ_1 is a constant that is chosen to satisfy the power constraint (3).

We then have proved that a time reversed precoding is optimum in terms of SNR, given $c_2(t) = p(-t)$.

C. Optimum Receiver Filter for Time Reversal System

We now consider another case. Given time reversal precoding, i.e., $C_1(f) = H^*(f)$, we wish to optimize the receiver filter $c_2(t)$ (maximizing SNR), under the fixed transmitted power constraint of

$$P_2 = \int_{-\infty}^{+\infty} |P(f) H^*(f)|^2 df. \quad (7)$$

The receiving SNR at the output of $c_2(t)$ can be expressed as

Similary, we refer to Schwartz inequality and have the SNR formulation,

$$SNR \leq \frac{2 \int_{-\infty}^{+\infty} |P(f) H^*(f) H(f)|^2 df}{N_0}, \quad (8)$$

with equality holding only when $C_2(f) = \lambda_2 P^*(f) H(f) H^*(f)$. It is suggested that the optimal receiver filter for a time reversal system should be a filter whose impulse response is in a form of $\lambda_2 p(-t) * h(t) * h(-t)$. This result is actually a validation of the matched filter theory.

D. Suboptimum Receiver Filter for Time Reversal System: One-correlator Receiver

Channel estimation is a difficult task and in a TR system this task is shifted to the transmitter side. We are interested in a suboptimum receiver filter, and the transfer function of which is matched to $P^*(f)$, instead of the optimum one $P(f)H(f)H^*(f)$. This case is exactly the scenario if we move the first channel matched filter $c_1(t)$ to the transmitter side, as discussed at the beginning of this Section. The following section is to study time reversal system performance with such a suboptimum receiver, namely, one-correlator receiver, firstly for a single antenna system, and later extended to a multiple antenna system.

The proposed scheme is suboptimal and of low complexity compared to many optimal criteria. Consider a joint optimization scenario, where $h(t)$ is given and we wish to find the optimum pair of $c_1(t)$ and $c_2(t)$, under the constraint of fixed transmitted power (denoted as P_2). If the signal has finite time duration, the optimum transmitted waveform is the eigenfunction corresponding to the maximum eigenvalue of the time reversal operator of the CIR $h(t)$ [43]. We should, however, note that other eigenvalues may contain significant information about the channel: thus putting as much as energy to just one frequency (to optimize in terms of SNR) may decrease channel capacity substantially—leading to low channel capacity. We still need implement water-filling algorithm to achieve the optimum capacity. When signal duration is infinite, $T = \infty$, this optimization leads to sinusoidal transmitted waveform, as shown in [42]. In other words, we need concentrate all the transmitted power to the frequency with maximum transmission capability.

III. PERFORMANCE ANALYSIS

A. System Description

Consider a single user transmission. The transmitted signals before precoding can be expressed as

$$s(t) = \sum_{i=-\infty}^{+\infty} s_i(t) = \sum_{i=-\infty}^{+\infty} \sqrt{E_b} b_i p(t - iT_b), \quad (9)$$

where E_b is the transmitted bit energy, $b_i \in \{\pm 1\}$ is the i -th information bit. Binary antipodal modulation has been considered in this paper. $p(t)$ is the UWB pulse with a width of T_p , and assume the pulse takes care of the impacts of circuits and antennas at the both sides. The energy of $p(t)$ is normalized to unity, i.e., $E_p = \int_{-\infty}^{+\infty} p^2(t) dt = 1$. T_b is the bit interval. Generally, we have $T_b \gg T_p$, in order to avoid the possible ISI caused by multipath channel. In this paper, we

will show that, by using a MIMO-TR technology, T_b and T_p could take the same level, without significant performance degradation.

For the sake of simplicity, we assume there is no per-path pulse distortion [37] caused by channel. If per-path pulse distortion does occur, a number of taps can be used to represent the per-path impulse response, as done in [39], such that the tap-delay-line (TDL) model in (10) is still valid in its mathematical form, but not physically interpreting the physics phenomenon. In this case, the received signals are just a series of replicas of the transmitted signals, with different attenuations and time delays. The CIR then can be modeled as

$$h(t) = \sum_{l=1}^L \alpha_l \delta(t - \tau_l), \quad (10)$$

where L is the number of multipath components and α_l and τ_l are their individual amplitudes and delays. Note that each term in (10) is not necessarily corresponding to a physical path.

B. Matched Filter Performance Bound

If there is no time reversal and a single antenna is employed at both the transmitter and the receiver, the received signal can be expressed as

$$r_i(t) = \sum_{l=1}^L \alpha_l s_i(t - \tau_l) + n(t). \quad (11)$$

The optimum receiver for the above signal would be a matched filter matched to the signal part of $r_i(t)$. Such a receiver would achieve the performance bound, namely matched filter bound, described as

$$P_e = Q \left(\sqrt{\frac{2GE_b}{N_0}} \right), \quad (12)$$

where $Q(x) = \int_x^\infty \frac{1}{\sqrt{2\pi}} e^{-y^2/2} dy$ is the Q-function and $G = \int_{-\infty}^{+\infty} |h(t)|^2 dt$ is the channel gain, and E_b represents the transmitted bit energy. The bit energy measured at the receiver side is denoted by \tilde{E}_b .

In reality, it is believed that the performance bound in (12), requires a very complex receiver and thus is hard to achieve, due to the complicated UWB multipath channel. In this section, we will show that, by using TR precoding at the transmitter, the AWGN performance bound can be achieved with a simple one-correlator receiver, under some conditions.

C. MISO-TR Performance Analysis based on Transmit Bit Energy E_b

Before we consider MIMO-TR, let us start with a simpler scenario of SISO-TR. Consider a non-realistic case where we use a short pulse so that the propagation delay difference between any adjacent multipath components is always larger than the pulse duration T_p . Also, we assume that T_b is sufficient enough so that there is no ISI.

For SISO-TR, the received signal can be expressed as

$$\begin{aligned} r_i^{SISO}(t) &= s_i(t) * c(t) * h(t) + n(t) \\ &= s_i(t) * \left\{ \frac{1}{\sqrt{G}} h(T-t) * h(t) \right\} + n(t) \\ &= s_i(t) * h_{eq}^{SISO}(t) + n(t) \end{aligned} \quad (13)$$

where $c(t) = h(T-t)/\sqrt{G}$ is the prefilter code, and $h_{eq}^{SISO}(t) = h(T-t) * h(t)/\sqrt{G}$ is the equivalent CIR for the SISO-TR scenario. It is apparent that $h_{eq}^{SISO}(t)$ is an autocorrelation with peak occurring at $t = T$. The magnitude of the peak is equal to \sqrt{G} , i.e., $h_{eq}^{SISO}(t = T) = \int_{-\infty}^{+\infty} |h(t)|^2 dt / \sqrt{G} = \sqrt{G}$.

Due to its autocorrelation nature, most of the energy is focused in the central (main) peak of the CIR $h_{eq}^{SISO}(t)$. Since we assume there are no Inter Pulse Interference (IPI), ISI and pulse distortion, we can use a filter matched to the main component of the received signal. It is proved in the following that even using such a simple receiver (with one correlator), we can achieve the same performance as the matched filter bound.

The main component of the receiving signal can be expressed as

$$r_i^{main}(t) = \sqrt{G} \sqrt{E_b} b_i p(t - iT_b - T). \quad (14)$$

We then use a filter matched to $p(t)$ to pick up the energy lying in the above main component of the received signal. The performance can be characterized using the following analytical formula,

$$P_e^{SISO} = Q \left(\sqrt{\frac{2GE_b}{N_0}} \right). \quad (15)$$

Comparing (15) and (12), it is evident that a TR system with one-correlator receiver can achieve the same performance as a system without TR but with an ideal matched filter. The same conclusion has been obtained by other researchers [35], [50], through different approaches in the Pre-rake systems. Therefore, for a TR system with one-correlator receiver, we have the following observation: On the one hand, TR filter improves the system performance by precoding

the transmitted signal so as to concentrate the transmitted power to the spectral regions with less attenuation and thus make more effective use of transmitted power; in contrast, system performance is degraded by use of non-optimum receiver (one-correlator receiver). Remarkably, the result in this Section implies that the improvement by placing a channel-matched TR filter at the transmitter is exactly equal to the degradation caused by not using such an optimum filter at the receiver. Again, this result is true, in the absence of ISI and IPI—a stringent condition.

In the following, we will extend this result to a scenario of TR with multiple antennas.

IV. MIMO-TR: FOCUSING SPATIAL-TEMPORAL ENERGY TO A SHARP PEAK

A. MIMO-TR Precoding

When a short pulse is sent to the channel, the radiated energy is distributed among different spatial locations and spread in time over a large number of pulses at any observation locations (due to multipath). Since a time reversal mirror—here antenna arrays at both MIMO terminals—can be viewed as a “channel sampler”, more antennas imply more spatial sampling points—more energy can be captured. A MIMO-TR (4×4) system configuration is illustrated in Fig. 2. Let $h_{mn}(t)$ denote the channel impulse response (CIR) between the m -th antenna at the transmitter and n -th antenna at the receiver, and $c_m(t)$ be the corresponding prefilter code employed in the m -th antenna branch at the transmitter. In a general $M \times N$ MIMO-TR system, the code $c_m(t)$ can be written as

$$c_m(t) = A_m \sum_{n=1}^N h_{mn}(T - t), \quad (16)$$

where T is the length of the filter required to implement the time reversal operation [21], and A_m is the power scaling factor to normalize the total transmission power from different antenna branches. It should be noted that different power allocation schemes can be implemented by choosing different factors A_m [25]. In this paper, A_m 's are set to be equal for all the antenna elements,

$$A_m = A = \frac{1}{\sqrt{\sum_{m=1}^M \sum_{n=1}^N G_{mn}}}, \quad (17)$$

where $G_{mn} = \int_{-\infty}^{+\infty} |h_{mn}(t)|^2 dt$ is the channel gain of CIR $h_{mn}(t)$.

To obtain the TR precoding waveform $c_m(t)$ for the m -th antenna branch is straightforward. First, a sounding pulse $w(t)$ is sent through all the N antennas in the receiver to the transmitter.

Secondly, the receiving signals at each transmitter antenna branch are then recorded, digitized and time reversed. The noise free signal received by the m -th antenna at the transmitter can be expressed as: $y_m(t) = \sum_{n=1}^N h_{mn}(t) * w(t)$. The foundation for using backward channel sounding is channel reciprocity. For MIMO channels, no experimental confirmation of this assumption has been done. If the sounding pulse $w(t)$ is sufficiently short, we can directly use the time reversed version of $y_m(T - t)$ as the precoding $c_m(t)$. Otherwise, deconvolution effort is necessary to remove the pulse effect from the received sounding signal.

One of the attractive characteristics of TR is that its temporal focal point can be adjusted by change of the parameter T . The principle of timing alignment for TR for the m -th antenna element is illustrated by Fig. 3. If the same initial timing between antenna elements in the same array is assumed (this is a reasonable assumption because all the antenna elements of an array use the same clock), all the peaks of the fields appear at the receiver at the same time instant, independently of the element location, antenna type, and channel. It turns out that the peaks are aligned automatically. For a MISO case, all the energy from different transmitter elements coherently adds up at time T , at the receive antenna. For MIMO case, energy from different transmitter elements (viewed as several different MISO arrays) will focus at each individual antenna element at the receiver.

For MIMO-TR, signal captured by the n -th receive antenna can be expressed as

$$r_i^n(t) = s_i(t) * \sum_{m=1}^M \{c_m(t) * h_{mn}(t)\} + n(t). \quad (18)$$

All the signals captured by different antennas at the receiver can be combined directly, and the combined signal $r_i(t)$ can be expressed as

$$\begin{aligned} r_i(t) &= s_i(t) * \sum_{n=1}^N \sum_{m=1}^M \{c_m(t) * h_{mn}(t)\} + n(t) \\ &= s_i(t) * A \sum_{n=1}^N \sum_{m=1}^M \left\{ \left[\sum_{k=1}^N h_{mk}(T - t) \right] * h_{mn}(t) \right\} \\ &+ n(t) \end{aligned} \quad (19)$$

$$\begin{aligned}
h_{eq}^{MIMO}(t) &= A \sum_{n=1}^N \sum_{m=1}^M \left\{ \left[\sum_{k=1}^N h_{mk}(T-t) \right] * h_{mn}(t) \right\} \\
&= A \underbrace{\sum_{n=1}^N \sum_{m=1}^M \left\{ \sum_{k=1, k \neq n}^N h_{mk}(T-t) * h_{mn}(t) \right\}}_{\text{Interference}} \\
&\quad + A \underbrace{\sum_{m=1}^M \sum_{n=1}^N R_{mn}(t-T)}_{\text{Signal}}
\end{aligned} \tag{20}$$

where $R_{mn}(t) = h_{mn}(-t) * h_{mn}(t)$ is the autocorrelation of $h_{mn}(t)$. Let us use a 4×4 MIMO example to illustrate (20). It can be seen from (20) that $h_{eq}^{MIMO}(t)$ consists of 64 terms, corresponding to 16 autocorrelations and 48 cross correlations. These 16 autocorrelation terms will coherently add up, due to its automatically alignment characteristic addressed in this section; In contrast, these 48 cross correlation terms adds up non-coherently. As a result, the desired autocorrelation part forms a strong peak and dominates in the received signal.

At $t = T$, the amplitude of the peak in h_{eq}^{MIMO} can be approximated by the contributions of all the autocorrelation terms as

$$A \sum_{m=1}^M \sum_{n=1}^N G_{mn} = \sqrt{\sum_{m=1}^M \sum_{n=1}^N G_{mn}}. \tag{21}$$

The signal on the main component of the received signal is then approximated as

$$r_i^{main}(t) \approx \sqrt{\sum_{m=1}^M \sum_{n=1}^N G_{mn}} \sqrt{E_b} b(i) p(t - iT_b - T) + n(t). \tag{22}$$

where \approx is used, because the contributions from all the cross correlation terms to the main peak have been ignored. In the absence of ISI and IPI, it follows that

$$P_e^{MIMO} = Q \left(\sqrt{2 \sum_{m=1}^M \sum_{n=1}^N G_{mn} E_b / N_0} \right). \tag{23}$$

Let \bar{G} denote the averaged channel gain over the whole $M \times N$ channels, $\bar{G} = \frac{1}{MN} \sum_{m=1}^M \sum_{n=1}^N G_{mn}$, we have

$$P_e^{MIMO} = Q(\sqrt{2MN\bar{G}E_b/N_0}). \tag{24}$$

As a special case when $N = 1$, we have performance of a MISO-TR system with one-correlator receiver

$$P_e^{MISO} = Q \left(\sqrt{2 \sum_{m=1}^M G_m E_b / N_0} \right). \quad (25)$$

When $M = 1, N = 1$, the equation (24) reduces to (15) for the SISO-TR scenario. It is straightforward from (25) that the performance of a MIMO-TR system depends on the following three parameters: the number of antennas M , N and the energy of the multipath (channel gain \bar{G}). Statistical characterization of \bar{G} is important.

B. Performance Analysis Based on the Receive Bit Energy \tilde{E}_b

The above analysis, e.g., (24), is based on the bit energy E_b on the transmitter side. Since a lot of literatures analyze the performance based on the receiver side bit energy \tilde{E}_b , this section also derives the performance formula for \tilde{E}_b . one-correlator receiver proposed in this paper is not optimum. The optimum receiver should be a receiver matched to the whole receive waveform of (24). Then, the performance bound for such a receiver would be the matched filter bound, expressed as $P_e = Q(\sqrt{\frac{2\tilde{E}_b}{N_0}})$ (assuming bi-polar modulation). We introduce a new metric, peak energy ratio κ , $\kappa = \frac{E_{peak}}{\tilde{E}_b}$, denoting the energy ratio of the peak to the total received energy. Here, E_{peak} represents the energy of the signal peak. As a result, the performance of one-correlator receiver can be expressed as $P_e = Q(\sqrt{\frac{2\tilde{E}_b\kappa}{N_0}})$.

Let $\nu_{mn,ij} = \int_{-\infty}^{+\infty} |h_{mn}(-t) * h_{ij}(t)|^2 dt - I_{mn,ij}$ for cross correlation ($m \neq i, n \neq j$) and $\nu_{mn,ij} = \nu_{mn} = G_{R_{mn}} - G_{mn}$ for autocorrelation ($m = i, n = j$). Here $I_{mn,ij} = |h_{mn}(-t) * h_{ij}(t)|_{t=0} = \int_{-\infty}^{+\infty} h_{mn}(t) \times h_{ij}(t) dt$, and $G_{R_{mn}} = \int_{-\infty}^{+\infty} |R_{mn}(t)|^2 dt$ is the channel gain of the equivalent CIR $R_{mn}(t)$. Here we can see that cross correlation $\nu_{mn,ij}$ represents the sidelobe energy of the equivalent CIR $h_{mn,ij}$.

For MIMO-TR, the peak energy ratio κ_{MIMO} can be written as

$$\begin{aligned} \kappa_{MIMO} &\approx \frac{(\sum_{m=1}^M \sum_{n=1}^N G_{mn} + \sum_{n=1}^N \sum_{m=1}^M \sum_{k=1, k \neq n}^N I_{mn, mk})^2}{2 \sum_{n=1}^N \sum_{m=1}^M \sum_{k=1, k \neq n}^N \nu_{mn, mk} + \sum_{m=1}^M \sum_{n=1}^N \nu_{mn} + (\sum_{m=1}^M \sum_{n=1}^N G_{mn} + \sum_{n=1}^N \sum_{m=1}^M \sum_{k=1, k \neq n}^N I_{mn, mk})^2} \\ &= \frac{[\bar{G} + (N-1)\bar{I}]^2}{\frac{2N-1}{MN} \bar{\nu} + [\bar{G} + (N-1)\bar{I}]^2} \end{aligned} \quad (26)$$

where $\bar{\nu} = 1/MN \cdot \sum_{m=1}^M \sum_{n=1}^N \nu_{mn}$, and $\bar{I} = 1/[MN(N-1)] \cdot \sum_{n=1}^N \sum_{m=1}^M \sum_{k=1, k \neq n}^N I_{mn,mk}$. Assuming that CIRs are not correlated with each other, i.e., $\bar{I} \approx 0$, then we have

$$\kappa_{MIMO} \approx \frac{\bar{G}^2}{\frac{2N-1}{MN}\bar{\nu} + \bar{G}^2} \quad (27)$$

for large N , we have

$$\kappa_{MIMO} \approx \frac{\bar{G}^2}{\frac{2}{M}\bar{\nu} + \bar{G}^2}. \quad (28)$$

For MISO-TR

$$\frac{(A \sum_{m=1}^M G_m)^2}{A^2 \sum_{m=1}^M \nu_m + (A \sum_{m=1}^M G_m)^2} = \frac{\bar{G}^2}{\frac{1}{M}\bar{\nu} + \bar{G}^2}. \quad (29)$$

For SISO-TR

$$\kappa = \frac{G^2}{\nu + G^2}. \quad (30)$$

As a sanity check, when $N = 1$, (27) reduces to MISO case (29). When $M = 1$ and $N = 1$, (27) reduces to SISO case (30).

It then can be seen from (28) and (29) that the performances of both the MIMO and MISO scenarios depend on the number of transmit antenna elements M . If we increase M , we actually improve the focusing and then get better performance. A comparison of (27) and (29) shows that peak energy ratio κ for a MISO system is better than a MIMO system, especially when N is large, the performance improvement caused by the increase of M for a MISO system is faster than that of a MIMO system.

V. MIMO-TR: SPATIAL MULTIPLEXING

A. Enhanced Spatial Focusing with Multiple Antennas

Let $h(\mathbf{r}_0, t)$ represent the CIR for the intended receiver located in the position $\mathbf{r}_0(x_0, y_0, z_0)$, and $h(\mathbf{r}_1, t)$ denote the CIR of another unintended user at the position $\mathbf{r}_1(x_1, y_1, z_1)$. The equivalent CIR for the intended user would be

$$h_{eq}(\mathbf{r}_0, \mathbf{r}_0, t) = h(\mathbf{r}_0, -t) * h(\mathbf{r}_0, t). \quad (31)$$

For the unintended user, the equivalent CIR would be

$$h_{eq}(\mathbf{r}_0, \mathbf{r}_1, t) = h(\mathbf{r}_0, -t) * h(\mathbf{r}_1, t). \quad (32)$$

The spatial focusing can be characterized by the metric directivity $D(\mathbf{r}_0, \mathbf{r}_1)$ defined as

$$D(\mathbf{r}_0, \mathbf{r}_1) = \frac{\max_t |h_{eq}(\mathbf{r}_0, \mathbf{r}_0, t)|^2}{\max_t |h_{eq}(\mathbf{r}_0, \mathbf{r}_1, t)|^2}. \quad (33)$$

For the scenario of MISO-TR, the equivalent CIR for different users can be expressed as

$$\begin{aligned} h_{eq}(\mathbf{r}_0, \mathbf{r}_0, t) &= \sum_{m=1}^M \frac{1}{\sqrt{M} \sqrt{\|h_m(\mathbf{r}_0, t)\|^2}} h_m(\mathbf{r}_0, -t) * h_m(\mathbf{r}_0, t) \\ h_{eq}(\mathbf{r}_0, \mathbf{r}_1, t) &= \sum_{m=1}^M \frac{1}{\sqrt{M} \sqrt{\|h_m(\mathbf{r}_0, t)\|^2}} h_m(\mathbf{r}_0, -t) * h_m(\mathbf{r}_1, t). \end{aligned} \quad (34)$$

where $h_m(\mathbf{r}_0, t)$ denotes the CIR between the m -th element in the transmit array and the receiver located in \mathbf{r}_0 .

For simplicity, the receiver has been restricted to move along a straight line in the measurements carried out in this paper. Under this condition, Eq. (33) can be simplified as

$$D(\mathbf{r}_0, d) = \frac{\max_t |h_{eq}(\mathbf{r}_0, 0, t)|^2}{\max_t |h_{eq}(\mathbf{r}_0, d, t)|^2}, \quad (35)$$

where d is the distance between the unintended receiver and the intended receiver (focal point) located at \mathbf{r}_0 . For the case where the antenna elements are not distributed along a line, but in some shapes (e.g., circle, square and etc.), (35) will still be valid if we replace the scalar d with a vector \mathbf{d} , where $\mathbf{d} = \mathbf{r}_1 - \mathbf{r}_0$.

The value of directivity $D(\mathbf{r}_0, d)$ determines how well we can, by employing TR, focus the transmitted energy into an intended point of interest. A similar metric has been used in [41]. Our previous paper [10] uses the same metric to investigate the spatial focusing of the UWB signal in the hallway environment by simulation. In this paper, we experimentally evaluate this parameter by moving the receiver away from the intended focusing point, \mathbf{r}_0 , and study how rapidly the receiving energy drops with this moving.

We expect the spatial focusing can be enhanced by employing multiple antennas at the transmitter, which will be shown experimentally in this paper. If the spatial focusing is good enough, we can take advantage of this property and transmit signals in a parallel fashion.

B. Spatial Multiplexing with Multiple Antennas

Consider a communication link consisting of M transmitting antennas and N receiving antennas. Input data are serial-to-parallel converted into N streams $b_n(t)$, which are precoded by $c_n(t)$

through FIR filters and modulated. Eventually the signals are sent to M transmitting antennas for simultaneous transmission. After the signal passes through the channel and is corrupted by AWGN, the n -th receiving branch extracts the data stream $b_n(t)$.

Let $\mathbf{S}(t) = [s_1(t), s_2(t), \dots, s_N(t)]$ and $\mathbf{R}(t) = [r_1(t), r_2(t), \dots, r_N(t)]$ denote the transmitting signal and receiving signal, respectively. We have $\mathbf{R}(t) = \mathbf{S}(t) * \mathbf{C}(t) * \mathbf{H}(t)$, here $\mathbf{C}(t)$ is the precoding matrix and $\mathbf{H}(t)$ is time domain impulse response matrix, defined by

$$\mathbf{H}(t) = \begin{bmatrix} h_{11}(t) & \dots & h_{1N}(t) \\ \vdots & \ddots & \vdots \\ h_{M1}(t) & \dots & h_{MN}(t) \end{bmatrix} \quad (M \times N) \quad (36)$$

We define the Equivalent Impulse Response Matrix (EIRM) as $\mathbf{H}_{eq}(t) = \mathbf{H}(t) * \mathbf{C}(t)$. Then we have $\mathbf{R}(t) = \mathbf{S}(t) * \mathbf{H}_{eq}(t)$. The EIRM is the target of interest. The objective is to transform the EIRM into a desirable form, by selecting a good code matrix $\mathbf{C}(t)$.

To avoid ISI, the ideal EIRM will be in a form of

$$\mathbf{H}_{eq}(t) = \begin{bmatrix} a_1\delta(t) & \dots & 0 \\ \vdots & \ddots & \vdots \\ 0 & \dots & a_n\delta(t) \end{bmatrix} \quad (N \times N) \quad (37)$$

where (a_1, \dots, a_n) are the matrix coefficients.

We hope we can find a matrix $\mathbf{C}(t)$ that satisfies the following equation:

$$\mathbf{C}(t) * \mathbf{H}(t) \approx \mathbf{H}_{eq}^{ideal}(t).$$

Then the problem will be how to find a suitable $\mathbf{C}(t)$. Two solutions can be used to achieve the goal:

1) *Solution 1: Inverse Filter:* This approach is optimal in the sense that, theoretically, the ideal formula presented above can be exactly achieved.

Thinking the problem in the frequency domain

$$\hat{\mathbf{C}}(f)\hat{\mathbf{H}}(f) = \hat{\mathbf{H}}_{eq}(f),$$

where $\hat{\mathbf{C}}(f)$, $\hat{\mathbf{H}}(f)$, and $\hat{\mathbf{H}}_{eq}(f)$ are the Fourier Transform of the matrices $\mathbf{C}(t)$, $\mathbf{H}(t)$ and $\mathbf{H}_{eq}(t)$ respectively.

The solution for above function is

$$\hat{\mathbf{C}}(f) = \hat{\mathbf{H}}_{eq}(f)\hat{\mathbf{H}}^{-1}(f).$$

The above solution assumes that the channel matrix $\mathbf{H}(f)$ is square and invertible. For a general $M * N$ matrix \mathbf{H} , the solution will be

$$\hat{\mathbf{C}}(f) = \hat{\mathbf{H}}_{eq}(f) \hat{\mathbf{H}}(f) \left(\hat{\mathbf{H}}^H(f) \hat{\mathbf{H}}(f) \right)^{-1}, \quad (38)$$

Once we have the frequency domain matrix $\mathbf{C}(f)$, the time domain matrix $\mathbf{C}(t)$ can be numerically obtained by applying IFFT to $\mathbf{C}(f)$. Note that transform of a matrix is a process of term by term transformation. Generally, the inversion of an matrix is ill-conditioned, small errors (e.g., the measurement error caused by noise) in any matrix \mathbf{X} will give rise to significant errors in its inverse matrix \mathbf{X}^{-1} . Even measurement is perfect and there is no error in \mathbf{X} , \mathbf{X} may not be invertible. Many techniques for the regularization of this problem have been studied [23].

2) *Solution 2: Time Reversal (TR)*: Considering the signal processing involved in the previous inverse filter solution, another simpler solution would be time reversal. In this case, the precoding matrix would simply be $\mathbf{C}_{TR}(t) = \mathbf{H}'(-t)$, where superscript “ ’ ” in the notation denotes transpose operation.

$$\mathbf{C}_{TR}(t) = \begin{bmatrix} h_{11}(-t) & \dots & h_{M1}(-t) \\ \vdots & \ddots & \vdots \\ h_{1N}(t) & \dots & h_{MN}(-t) \end{bmatrix} \quad (N \times M) \quad (39)$$

In practice, $\mathbf{C}_{TR}(t)$ can be readily obtained by channel sounding and no extra computation is needed.

Let $\mathbf{H}_{eff}(t) = \mathbf{C}_{TR}(t) * \mathbf{H}(t)$,

$$\mathbf{H}_{eff}(t) = \begin{bmatrix} \sum_{i=1}^M R_{h_{i1}}(t) & \dots & \sum_{i=1}^M h_{i1}(-t) * h_{in}(t) & \dots & \sum_{i=1}^M h_{i1}(-t) * h_{iN}(t) \\ \vdots & \ddots & \vdots & & \vdots \\ \sum_{i=1}^M h_{in}(-t) * h_{i1}(t) & \dots & \sum_{i=1}^M R_{h_{in}}(t) & \dots & \sum_{i=1}^M h_{in}(-t) * h_{iN}(t) \\ \vdots & & \vdots & \ddots & \vdots \\ \sum_{i=1}^M h_{iN}(-t) * h_{i1}(t) & \dots & \sum_{i=1}^M h_{iN}(-t) * h_{in}(t) & \dots & \sum_{i=1}^M R_{h_{iN}}(t) \end{bmatrix} \quad (N \times N) \quad (40)$$

Here we have made an assumption that matrix convolution is term by term convolution.

In a general form, the received signal $\mathbf{r}(t)$ can be expressed as

$$r_n(t) = \sum_{j=1}^N s_j(t) * \left[\sum_{i=1}^M h_{ij}(-t) * h_{in}(t) \right], \quad n = 1, 2, \dots, N \quad (41)$$

The received signal $\mathbf{r}(t)$ can be reformulated to a more convenient form,

$$r_n(t) = s_n(t) * \sum_{i=1}^M R_{h_{in}}(t) + O_n(t), \quad n = 1, 2, \dots, N \quad (42)$$

where $O_n(t) = \sum_{j=1, j \neq n}^N s_j(t) * \left[\sum_{i=1}^M h_{ij}(-t) * h_{in}(t) \right]$.

Assuming good spatial focusing, the received signal can be approximated by the following formula $r_n(t) \approx s_n(t) * \sum_{i=1}^M R_{h_{in}}(t)$, where we have ignored the contributions from the cross correlation part $O_n(t)$. Under this condition, the corresponding impulse response matrix will be in the form of a diagonal matrix

$$\mathbf{H}_{eff}(t) = \begin{bmatrix} \sum_{i=1}^M R_{h_{i1}}(t) & \dots & 0 \\ \vdots & \ddots & \vdots \\ 0 & \dots & \sum_{i=1}^M R_{h_{iN}}(t) \end{bmatrix} \quad (N \times M) \quad (43)$$

where the impulse matrix has been decomposed into parallel channels. This decomposition gives us several independent sub-channels, and thus increases the data rate.

Time reversal spatial multiplexing discussed in this section is another application of TR-MIMO, in addition to the application of beamforming. The precodings for the two different scenarios are different. As a sanity check, in the following we will show that scenario A (spatial multiplexing) is reduced to scenario B (beamforming), when all the independent channels transmit the same information, namely, $s_n(t) = s_{com}(t)$.

Under this condition, the receiving signal can be combined together directly and is expressed as

$$\begin{aligned} r(t) &= \sum_{n=1}^N r_n(t) \\ &= \sum_{n=1}^N \left[\sum_{j=1}^N s_{com}(t) * \left(\sum_{i=1}^M h_{ij}(-t) * h_{in}(t) \right) \right] \\ &= s_{com}(t) * \sum_{m=1}^N \sum_{j=1}^N \left[\sum_{i=1}^M h_{ij}(-t) * h_{im}(t) \right] \\ &= s_{com}(t) * \sum_{j=1}^N \left[\sum_{i=1}^M h_{ij}(-t) * \sum_{m=1}^N h_{im}(t) \right]. \end{aligned} \quad (44)$$

The equivalent impulse response thus can be modeled as

$$h_{eq}^{MIMO}(t) = \sum_{j=1}^N \left(\sum_{i=1}^M h_{ij}(-t) * \sum_{m=1}^N h_{im}(t) \right).$$

Considering power allocation factor A , we have

$$h_{eq}^{MIMO}(t) = A \sum_{j=1}^N \left(\sum_{i=1}^M h_{ij}(-t) * \sum_{m=1}^N h_{im}(t) \right),$$

which is consistent with the result derived previously in (20).

VI. UWB SPATIAL CHANNEL MEASUREMENT

A. Experiment Setup

Major equipment used in the measurements includes: (1) a waveform generator for triggering the pulser; (2) a UWB pulser that generates Gaussian like pulses with RMS pulse width of approximate 250 ps; (3) a wideband low noise amplifier (LNA) with bandwidth over 10 GHz and noise figure less than 1.5 dB; (4) a Tektronix CSA8000 Digital Sampling Oscilloscope (DSO) with a 20 GHz sampling module 80E03; and (5) a pair of omni-directional antennas with relatively flat gain over the signal band. To maintain synchronization, the same waveform generator is employed to trigger the DSO. The major frequency components of the system are from 750 MHz to 1.6 GHz. A simplified block diagram of the experiment setup can be found in Fig. 4.

A virtual antenna array is employed in the experiments. The elements of the array are spaced far enough so that there is no significant correlation between two adjacent channels. This can be achieved by setting the spacings between any two adjacent antenna elements greater than 20 cm, which corresponds to the half wavelength of the lowest frequency. The value of 20 cm is found to be sufficient after some trials of bigger values. The MIMO antenna coupling is considered in [18]. In Fig. 5, four virtual elements are equally spaced along a line. The heights of the antennas are set to 1.4 m. The receiving antenna is moved to different locations, and individual channels were sounded and measured sequentially. No Line of Sight (LOS) is available for all the measurements.

B. Experiment Environment

A set of measurements have been performed in the office area of Clement Hall 400 at Tennessee Technological University. Fig. 5 shows the experimental layout for these experiments. In Fig. 5 (also in Table I), T_n denotes the n -th element of the transmitting array and R_n the receiver located in the n -th position. The environment for the experiment is a typical office area with abundance of wooden and metallic furniture (chairs, desks, bookshelves and cabinets).

C. Measurement Results and Spatial Focusing Analysis

A typical receiving waveform is shown in Fig. 6. The CLEAN algorithm is employed to extract CIRs from the received waveforms.

We first investigate the spatial focusing of a MISO-TR system. Consider downlink transmission. Assume there are two users separated by a distance d , with one of them as the target user (focal point) and the other one as the undesired user. Each user has one receive antenna and a transmit antenna array with four elements. The equivalent CIRs for the target user and the undesired user of 0.2 m away are shown in Fig. 7(a) and Fig. 7(b), respectively. The equivalent CIRs for different users are calculated by using (34). As we can see from Fig. 7, the signal is very strong for the target user while it is almost behind the background noise for the undesired user with a short distance of 0.2 m away.

We further investigate the variation of the directivity D , defined in Section V-A, with respect to different distances d . A comparison of spatial focusing for MISO-TR and SISO-TR is shown in Fig. 8. In the SISO-TR case, it is observed that energy drops more than 15 dB when the undesired receiver is located 0.2 m away from the intended user. This number will slightly change when the unintended receiver moves to a farther place. In Fig. 8, the ‘‘SISO average’’ curve represents the average directivity of the four SISO-TR cases. It is observed that the ‘‘MISO’’ directivity curve drops much faster than the ‘‘SISO average’’ curve, implying that spatial focusing is improved by employing antenna array at the transmitter. With a four-element array at the transmitter, energy drops 22 dB when the unintended receiver is 0.2 m away from the target receiver.

VII. NUMERICAL RESULTS

Table I shows a comparison of κ (defined in Section IV-B) for different scenarios. In Table I, the calculating of parameters ν , G^2 , κ are all based on measured UWB spatial channels. The

approximated (“Appro”) values of κ for MIMO and MISO scenarios are calculated using the formulas (28) and (29), respectively. The experiment (“Exper”) values are directly measured from the equivalent CIRs of MISO and MIMO scenarios. Table I shows that the formulas (28) and (29) can approximate the measured value well. The slight difference between the approximated value and the measured value is due to the disturbances of the cross correlation terms (the interference from the other antennas), which is hard to be included in an analytical formula.

Based on the measured UWB spatial channels, we conduct Monte Carlo simulations to investigate the performance of one-correlator receiver and compare them under different scenarios: SISO, MISO, and MIMO. In our simulation, the second order derivative of Gaussian pulse has been used as the transmitted pulse $p(t)$, which is mathematically defined as:

$$p(t) = \left[1 - 4\pi \left(\frac{t - t_c}{w} \right)^2 \right] e^{-2\pi \left(\frac{t - t_c}{w} \right)^2} \quad (45)$$

where w is the parameter controlling the width of the pulse (and therefore the frequency bandwidth of the transmit signal), and t_c is the parameter to shift the pulse to the middle of the window. In the following simulation, we let $w = 1$ ns and $t_c = 0.5$ ns. To avoid the presence of severe ISI in the system, we add an inter-pulse guard time T_g . Therefore, we have $T_b = w + T_g$. Moreover, T_g can be used to adjust the transmission data rate in the simulation. Unless stated otherwise, we let $T_g = w$, corresponding to a data rate of 500 Mb/s.

Throughout the paper, we assume perfect synchronization and the transmitter has the full knowledge of the channel information. To make the comparison fair, performances of SISO and MISO scenarios have been averaged over all the corresponding specific channels that virtually form the MIMO channel, i.e., $P_{ave}^{SISO} = \frac{1}{16} \sum_{i=1}^{16} P_i^{SISO}$, and $P_{ave}^{MISO} = \frac{1}{4} \sum_{i=1}^4 P_i^{MISO}$.

A comparison of BER performance for different scenarios with both ISI and IPI is shown in Fig. 9. The performance bound for AWGN channel is also plotted as a reference. From Fig. 9 we can see that, given the same SNR at the receiver side, MISO-TR has the best performance, and MIMO-TR is slightly better than SISO-TR scenario. This is due to the best temporal focusing provided by MISO-TR. It should be noted that these comparisons are based on the received SNR. In reality, however, given the same transmitted power, the SNR at the receiver side for MIMO-TR is much higher than that of MISO-TR, which will make MIMO-TR outperform MISO-TR, as will be illustrated in the following.

Fig. 10 shows the BER performances for the SISO, MISO, and MIMO scenarios, under the

same transmitted power constraint, with different transmission data rates. For the MIMO scenario, all the four antennas transmit the same bit information, i.e., the beamforming approach has been applied to increase the SNR at the receiver side. Both IPI and ISI have been considered. As we can see from Fig. 10, MIMO-TR outperforms MISO-TR and then MISO-TR outperforms SISO-TR. Tests were conducted for data rates of 500 Mb/s and 225 Mb/s. As expected, an increase in the data rate leads to a performance degradation. For a data rate of 250 Mb/s, about 13 dB power gain (compared with SISO-TR) is achieved by employing a 4×4 MIMO array. The power gain in a system with ISI and IPI is slightly higher than the theoretical power gain $10\log_{10}(\text{MN})$, derived in Section IV-A, where we assume there are no ISI and IPI.

To illustrate the concept of spatial multiplexing for MIMO-TR, we study a simple scenario of 2×2 MIMO-TR system. As stated in Section V, the signal will first be serial-to-parallel converted into two streams, precoded with TR precoding and then sent to two transmitting antennas for simultaneous transmission. The signal passes through the channel and is corrupted by AWGN. Fig. 11 shows the BER performance for the two parallel sub-channels. Compared to beamforming approach addressed previously, one more interference source from inter channels need to be considered in the spatial multiplexing simulation.

VIII. CONCLUSIONS

Time reversal is considered in the framework of UWB MIMO. Experimental measurements have been used to evaluate the performance. Multiple antennas are found to be very useful in a UWB system. The working principles for MIMO in a UWB system is fundamentally different from that for a narrowband, flat fading wireless system. The fading is not a concern for UWB communications. The leading mechanism behind UWB MIMO is to exploit the space-time focusing that is unique to an impulse signal. The design philosophy is to use deterministic signal model as Digital Subscriber Line (DSL), rather than the statistic fading signal in a narrowband system. This reported work is the first step toward the non-fading transmission [20], for UWB systems. The time reversed MIMO matrix is combined with the physical channel, to form an effective matrix channel that can be treated deterministically [20].

One feasible scheme of combining the MIMO with the one-finger correlator has been demonstrated. Some further simplification of the transceiver can be done using a chirp UWB system. When a pair of chirp waveforms in the transmitter and receiver is used to replace the second

order Gaussian pulse as the modulation waveform, the new scheme may prove to be useful for some high-data rate communications with a relatively low cost [17], [19]. What we have learned from the past is that too many multipath fingers force us to walk away from the famous RAKE structure to reduce the transceiver cost. For example, for a transmitted pulse of one nanosecond, a dense multipath spread of 1000 ns is observed in a metal cavity in [17], [19], it is believed that time reversal is necessary to capture the spread multipath energy. As suggested in this paper, the MIMO transmission with time reversal can be further used to make full use of the space-time channel responses at the same time. The work reported here, thus, paves the way for potentially solving the communication problem in some RF harsh environments like a metal cavity.

IX. ACKNOWLEDGMENT

We want to thank Drs. Brian Sadler, Santanu K. Das, and Robert Ulman for helpful discussions. We thank the anonymous reviewers for their thorough reading of the manuscript and the constructive suggestions. This work is funded by the Office of Naval Research through a grant (N00014-07-1-0529), National Science Foundation through a grant (ECS-0622125), the Army Research Laboratory, and the Army Research Office through a STIR grant (W911NF-06-1-0349), and a DURIP grant (W911NF-05-1-0111).

REFERENCES

- [1] R. Scholtz, "Multiple Access with Time-hopping Impulse Modulator (invited paper)," in *MILCOM'93*, pp. 11–14, October 1993.
- [2] M. Win and R. Scholtz, "Ultra-wide Bandwidth Time-hopping Spread Spectrum Impulse Radio for Wireless Multiple-access Communications," *IEEE Trans. Commun.*, vol. 48, pp. 679–689, April 2000.
- [3] S. Roy, J. Foerster, V. Somayazulu, and D. Leeper, "Ultra-wideband Radio Design: The Promise of High-speed, Short Range Wireless Connectivity," in *Proceedings of the IEEE*, vol. 92, pp. 295–311, February 2004.
- [4] R. C. Qiu, R. Scholtz, and X. Shen, "Ultra-Wideband Wireless Communications— A New Horizon," *IEEE Trans. Veh. Technol., Editorial on Special Issue on UWB*, vol. 54, September 2005.
- [5] R. C. Qiu, H. P. Liu, and X. Shen, "Ultra-Wideband for Multiple Access," *IEEE Commun. Mag.*, vol. 43, pp. 80–87, February 2005.
- [6] L. Yang and G. B. Giannakis, "Ultra-Wideband Communications: An Idea whose Time has Come," *IEEE Signal Processing Magazine*, vol. 21, no. 6, pp. 26–54, November 2004.
- [7] X. Shen, M. Guizani, H. Chen, R. C. Qiu, and A. Molisch, "Ultra-wideband Wireless Communications," *IEEE J. Select. Areas Commun., Editorial on Special Issue on UWB*, vol. 24, 2nd Quarter 2006.
- [8] M. Fink, "Time reversed acoustics," *Physics Today*, pp. 34–40, Mar. 1997.

- [9] T. Strohmer, M. Emami, J. Hansen, G. Papanicolaou, A. J. Paulraj, "Application of time-reversal with MMSE equalizer to UWB communications," *Proc. IEEE Global Telecommunications Conference*, vol.5 pp. 3123-3127, 2004.
- [10] C. Zhou and R. C. Qiu, "Spatial focusing of time-reversed UWB electromagnetic waves in a hallway environment," Submitted to *IEEE 38th Southeastern Symposium on System Theory*, Cookeville, TN, USA. March 5-7, 2006.
- [11] C. Oestges, *et al.*, "Characterization of space-time focusing in time-reversed random fields," *IEEE Trans. On Antennas and Propagat.*, Vol. 53, No. 1, pp. 283-293, Jan. 2005.
- [12] C. Zhou and R. C. Qiu, "Spatial Focusing of Time-Reversed UWB Electromagnetic Waves in a Hallway Environment," in *System Theory, 2006 Proceeding of the Thrity-Eighth Southeastern Symposium on*, pp. 318-322, 2006.
- [13] R. C. Qiu, C. Zhou, N. Guo, and J. Q. Zhang, "Time Reversal with MISO for Ultra-Wideband Communications: Experimental Results," *IEEE Antenna and Wireless Propagation Letters*, vol. 5, no. 1, pp. 269-273, 2006.
- [14] R. C. Qiu, "A Theory of Time-Reversed Impulse Multiple-Input Multiple-Output (MIMO) for Ultra-Wideband (UWB) Communications (invited paper)," in *2006 Int'l Conf. UWB*, October 2006.
- [15] R. C. Qiu, C. Zhou, J. Q. Zhang, and N. Guo, "Channel Reciprocity and Time-Reversed Propagation for Ultra-Wideband Communications," in *IEEE AP-S International Symposium on Antennas and Propagation, Honolulu, Hawaii*, vol. 1, June 2007.
- [16] C. Zhou, B. M. Sadler, and R. C. Qiu, "Performance Study on Time Reversed Impulse MIMO for UWB Communications Based on Realistic Channels," in *IEEE Conf. Military Comm., MILCOM'07*, (Orlando, FL), October 2007.
- [17] R. C. Qiu, B. M. Sadler, and Z. Hu, "Time Reversed Transmission with Chirp Signaling for UWB Communications and Its Application in Confined Metal Environments," in *International Conference on Ultra-wideband, ICUWB'07*, (Singapore), September 2007.
- [18] M. Calderon and R. C. Qiu, "Time Reversal for Ultra-wideband (UWB) Sensor Networking," tech. rep., Final Report to Army Research Office, Grant no. W911NF-06-1-0349, 151 pages, TTU, Cookeville, TN, July 2007.
- [19] R. C. Qiu and et al, "Ultra-wideband Communications Systems and Testbed," tech. rep., Final Report to Army Research Office, Grant no. W911NF-05-01-0111, 240 pages, TTU, Cookeville, TN, July 2007.
- [20] R. C. Qiu and et al, "Time-Reversal Based Range Extension Technique for Ultra-wideband (UWB) Sensors and Applications in Tactical Communications and Networking," Technical Report (Quarterly) to Office of Naval Research (ONR), Contract no. N00014-07-1-0529, 151 pages, TTU, Cookeville, TN, October 2007.
- [21] C. Zhou, N. Guo, and R. C. Qiu, "Experimental results on Multiple-Input Single-Output (MISO) time reversal for UWB systems in an office environment," *Military Communications Conference (MILCOM06)*, Washington DC, Oct. 2006.
- [22] D. Chambers, J. Candy *et al.*, "Time reversal and the spatio-temporal matched filter (L)," *J. Acoust. Soc. Am.*, Vol. 116, No. 3, pp. 1348-1350. Sept. 2004.
- [23] M. Tanter, J. Thomas, and M. Fink, "Time reversal and the inverse filter," *J. Acoust. Soc. Am.* Vol. 108, 223-234, 2000.
- [24] R. C. Qiu, C. Zhou, N. Guo, J. Q. Zhang, "Time reversal with MISO for Ultra-Wideband communications: experimental results," *IEEE Antennas and Wireless Propagation Letters*, pp. 269-273, Vol. 5, 2006.
- [25] P. Kyristi, G. Panicolaou, A. Oprea, "MISO time reversal and delay-spread compression for FWA channels at 5 GHz," *IEEE Antennas And Wireless Propagation Letters*, vol. 3, pp. 96-99, Dec. 2004.
- [26] R. Daniels and R. Heath, "Improving on time reversal with MISO precoding," *Proceedings of the Eighth International Symposium on Wireless Personal Communications Conference*, Aalborg, Denmark, September 18-22, 2005.
- [27] J.H. Winters, "On the capacity of radio communication systems with diversity in a Rayleigh fading environment," *IEEE Journal on Selected Areas in Communications*, Vol. 5, pp. 871-878. June 1987.

- [28] G.J. Foschini and M. Gans, "On limits of wireless communication in a fading environment when using multiple antennas," *Wireless Personal Commn.*, pp. 311-335, March, 1998.
- [29] Wipawee Siriwongpairat, "Cross-layer design for multi-antenna ultra-wideband systems," Ph.D. dissertation, Department of Electrical and Computer Engineering, University of Maryland, College Park, 2005.
- [30] L. Wang, W. Liu, and K. Shieh, "On the Performance of Using Multiple Transmit and Receive Antennas in Pulse Based Ultra-Wideband Systems," *IEEE Transactions on Wireless Communications*, Vol. 4, no. 6, pp. 2738-2750, Nov. 2005.
- [31] W. Malik and D. Edwards, "Measured MIMO Capacity and Diversity Gain With Spatial and Polar Arrays in Ultrawideband Channels," *IEEE Transactions on Communications*, Vol. 55, no. 12, pp. 2361-2370, Dec. 2007.
- [32] R. Aiello, "Discrete Time PHY Proposal for TG3a," *Tech. Rep. IEEE 802.15-03/099r1*, March, 2003.
- [33] R. C. Qiu, "A Theory of Time-Reversed Impulse Multiple-Input Multiple-Output (MIMO) for Ultra-Wideband (UWB) Communications," invited paper, *IEEE International Conf. Ultra Wideband (ICUWB06)*, Boston, MA, Sept. 2006.
- [34] A. Sibille, "Time-Domain diversity in Ultra-Wideband MIMO communications," *EURASIP Journal on Applied Signal Processing*, Vole. 3, pp. 316-327, 2005.
- [35] S. Zhao and H. Liu, "Prerake diversity combining for pulsed UWB systems considering realistic channels with pulse overlapping and narrowband interference," in *IEEE GLOBECOM*, pp. 3784-3788, Nov. 2005.
- [36] H. Liu, R.C. Qiu, and Z. Tian, "Error Performance of Pulse-Based Ultra-Wideband MIMO Systems over Indoor Wireless Channels," *IEEE Trans. Wireless Communications*, Vol. 4, No. 6, pp. 2939-2944, Nov. 2005.
- [37] R. C. Qiu, "A Generalized Time Domain Mutlipath Channel and its Applications in Ultra-wideband (UWB) Wireless Optimal Receiver Design," *IEEE Trans. Wireless Communications*, Vol. 3, No. 11, pp. 2312-2324, Nov. 2004.
- [38] L. B. Felsen, and N. Marcuvitz, *Radiation and Scattering of Waves*, Prentice Hall, Upper Saddle River, NJ, 1973.
- [39] R. C. Qiu, J. Q. Zhang, and N. Guo, "Detection of Physics-Based Ultra-Wideband Signals Using Generalized RAKE and Multi-User Detection (MUD)," *IEEE J. Selected Areas in Commun. (JSAC), the Second JSAC special issue on UWB Radio*, vol. 24, May 2006.
- [40] H. T. Nguyen, J.B. Andersen, G. G. Pedersen, "The potential use of time reversal techniques in multiple element antenna systems," *IEEE Communication Letters*, vol. 9, No. 1, pp. 40-42. Jan. 2005.
- [41] S. M. Emami, J. Hansen, A .D. Kim, G. Papanicolaou, A. J. Paulraj, D. Cheung, and C. Prettie, "Predicted time reversal performance in wireless communications using channel measurements," *IEEE Communication Letters*, 2004.
- [42] E. J. Badhdady, *Lectures on communications system theory*, Ch. 14, 1961, New York: McGraw-Hill.
- [43] M. R. Bell, "Information theory and radar waveform design," *IEEE Trans. on Inf. Theory*, Vol., 39, No. 5, pp. 1578-1597, Sept. 1993.
- [44] H. T. Nguyen, I.Z.K. Kovacs, P.C.F. Eggers, "A Time Reversal Transmission Approach for Multi-user UWB Communications," Special Issue of *IEEE Transactions on Antennas Propagation on Wireless Communications*, vol. 54, nr. 11, pp. 3216-3224, 2006.
- [45] H. T. Nguyen, I.Z.K. Kovacs, P.C.F. Eggers, "A time reversal transmission potential for multiuser UWB communications," *IEEE Transactions on Antennas and Propagations*, pp. 1-13, 2005.
- [46] H. T. Nguyen, P. Kyritsi, P.C.F. Eggers, "Time Reversal Technique for Multi-user Wireless Communication with Single Tap Receiver," *Proceedings of the 16th IST Mobile and Wireless Communications Summit*, pp.. 1-5, 2007.
- [47] H. T. Nguyen, J.B. Andersen, G.F. Pedersen, P. Kyritsi, P.C.F. Eggers, "Time Reversal in Wireless Communications : A measurement-based investigation," *IEEE Transactions on Wireless communications*, vol. 5, nr. 8, pp. 2242-2252, 2006.

- [48] R. J. Cramer, "An evaluation of ultrawideband propagation channels," *PhD Dissertation*, University of Southern California, California, USA. Dec. 2000.
- [49] R. M. Buehrer *et al.*, " Ultra-wdeband propagation measurements and modeling final report," *DARPA NETEX program*, pp. 333- , Virginia Polytechnic Institute and State University, VA, USA. Jan. 2004.
- [50] R. Esmailzadeh, E. Sourour and M. Nakagawa, "Prerake combining in time-division duplex CDMA mobile communications," *IEEE. Tran. Veh. Techn.*, Vol 48, pp. 795-801, May 1999.

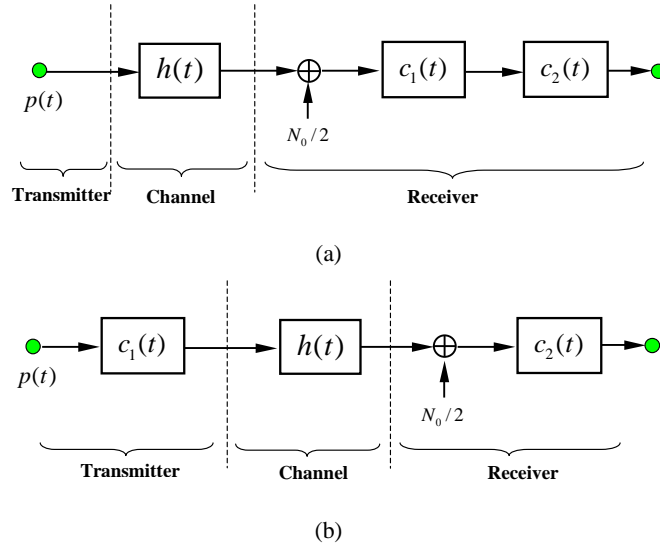


Fig. 1. Block diagram of the optimum transceiver design. (a) Matched Filter (b) Time Reversal

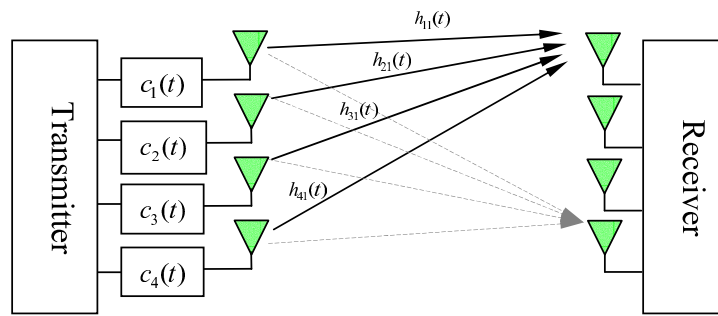


Fig. 2. Time reversal precoded MIMO communication system with $M = 4$ and $N = 4$.

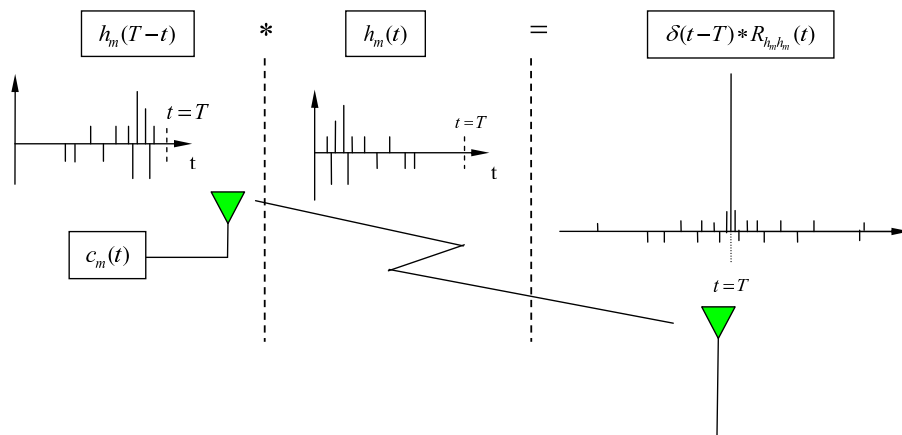


Fig. 3. Timing illustration for the peak of the received signal in a TR system. The peak of the equivalent CIR will occur exactly at the time $t = T$, independent of the element location, antenna type and channel.

	<i>Channel</i>	ν	G^2	κ
SISO-TR	T ₁ R ₁	0.0459	0.0483	0.5124
	T ₁ R ₂	0.0414	0.0454	0.5230
	T ₁ R ₃	0.0485	0.0467	0.4906
	T ₁ R ₄	0.0572	0.0581	0.5040
	T ₂ R ₁	0.0516	0.0512	0.4979
	T ₂ R ₂	0.0446	0.0413	0.4810
	T ₂ R ₃	0.0457	0.0455	0.4991
	T ₂ R ₄	0.0556	0.0477	0.4615
	T ₃ R ₁	0.0562	0.0543	0.4915
	T ₃ R ₂	0.0363	0.0355	0.4944
	T ₃ R ₃	0.0346	0.0367	0.5148
	T ₃ R ₄	0.0454	0.0451	0.4983
	T ₄ R ₁	0.0502	0.0485	0.4916
	T ₄ R ₂	0.0462	0.0445	0.4906
	T ₄ R ₃	0.0595	0.0573	0.4907
	T ₄ R ₄	0.0366	0.0369	0.5020
	Average	0.0472	0.0464	0.4965
MISO-TR	T ₁₂₃₄ R ₁	0.0577	0.2022	<i>Appro</i> : 0.8044
				<i>Exper</i> : 0.7781
	T ₁₂₃₄ R ₂	0.0493	0.1663	<i>Appro</i> : 0.7900
				<i>Exper</i> : 0.7714
	T ₁₂₃₄ R ₃	0.0520	0.1851	<i>Appro</i> : 0.7992
				<i>Exper</i> : 0.7807
	T ₁₂₃₄ R ₄	0.0605	0.1865	<i>Appro</i> : 0.7955
				<i>Exper</i> : 0.7552
	Average	0.0549	0.1850	<i>Appro</i> : 0.7977
				<i>Exper</i> : 0.7713
MIMO-TR	T ₁₂₃₄ R ₁₂₃₄	0.6401	0.6781	<i>Appro</i> : 0.5680
				<i>Exper</i> : 0.5144

TABLE I
A COMPARISON OF κ FOR DIFFERENT SCENARIOS

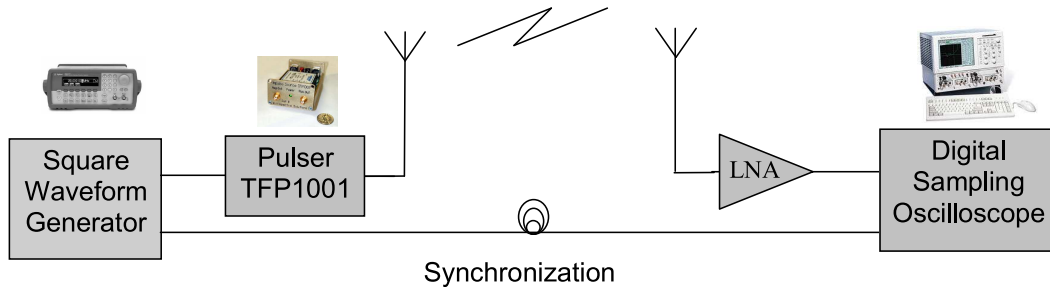


Fig. 4. UWB spatial channel measurement: experiment setup

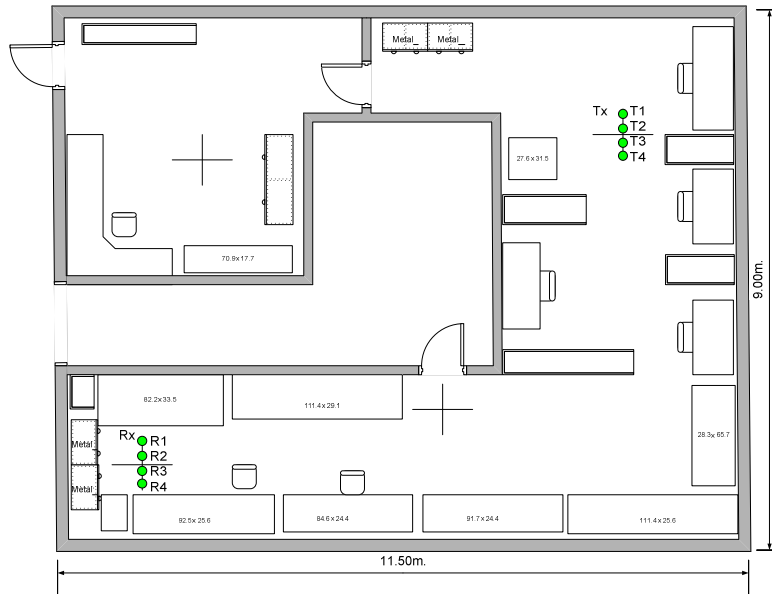


Fig. 5. UWB spatial channel measurement: experiment environment.

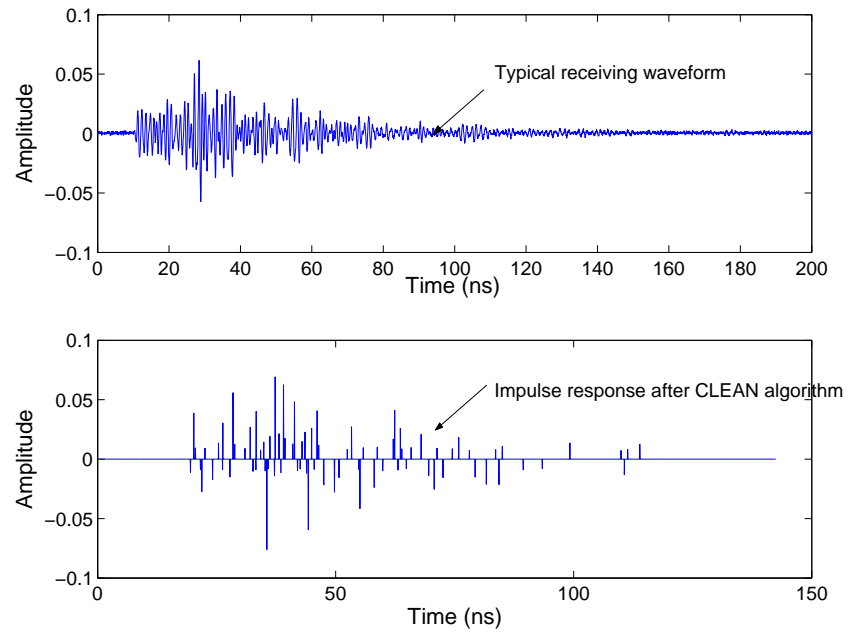


Fig. 6. CLEAN Algorithm is employed to extract impulse response from the received signals.

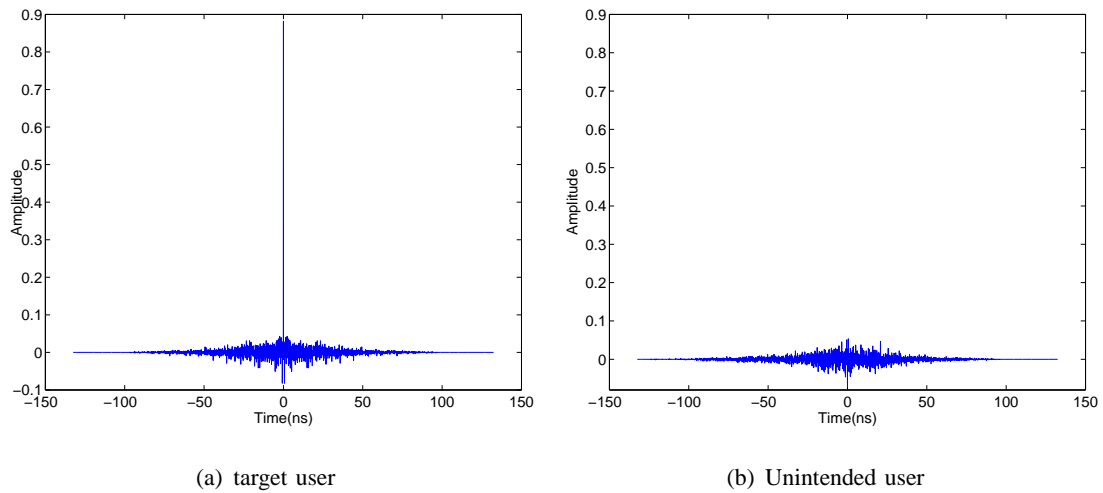


Fig. 7. Demonstration of MISO-TR spatial focusing by the equivalent CIR. (a) is the equivalent CIR for the target user. (b) is the equivalent CIR for the unintended user with 0.2 m away from the target user.

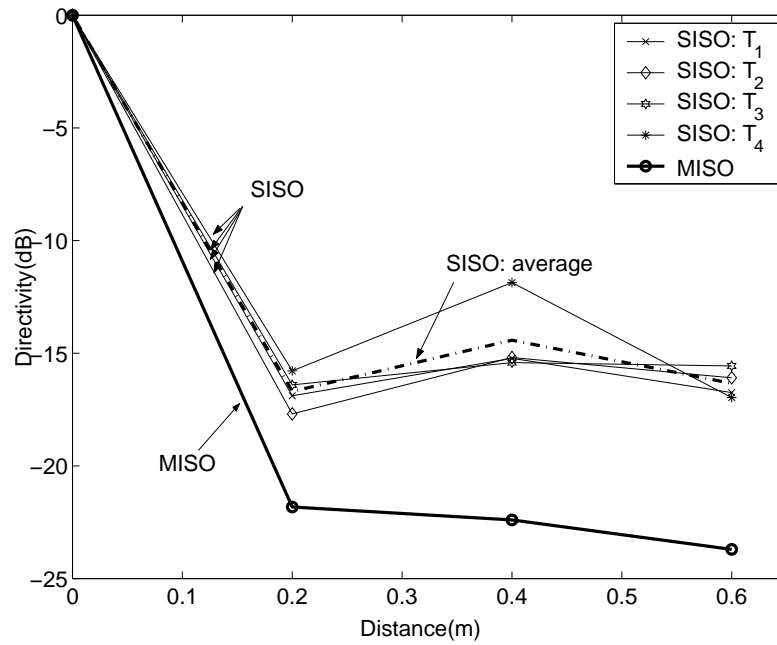


Fig. 8. Spatial focusing characterized by the parameter directivity $D(\mathbf{x}_0, d)$.

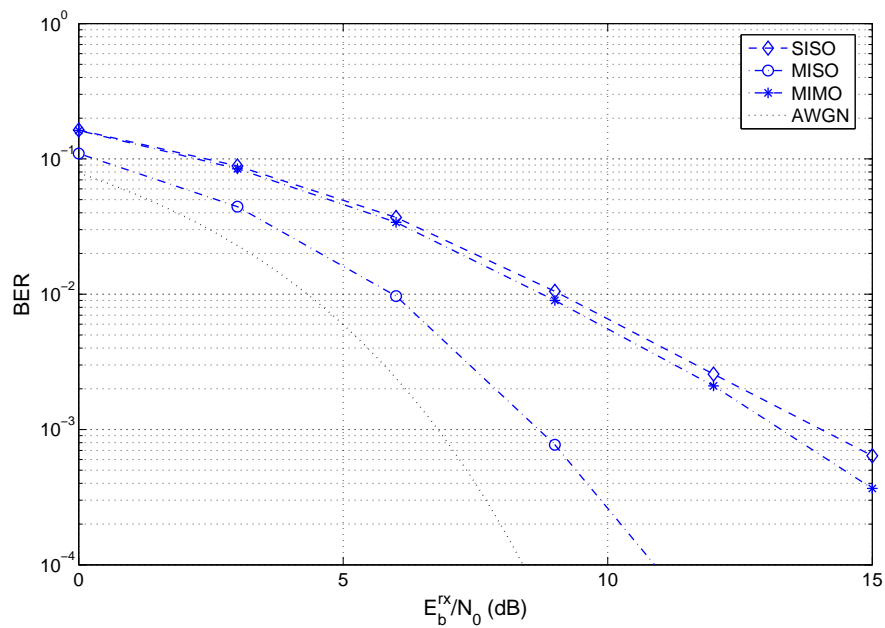


Fig. 9. BER performance in terms of received bit energy. IPI and ISI have been considered. SISO result is the average of 16 channels and MISO is the average of 4 channels.

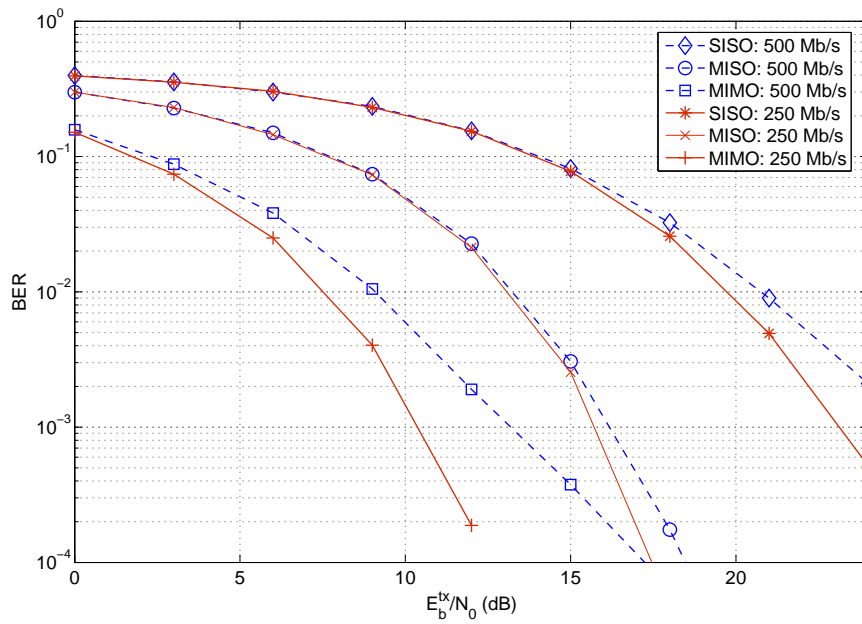


Fig. 10. BER performance in terms of transmitted bit energy. E_b^{tx} here represents the transmitted bit energy. Both ISI and IPI have been considered.

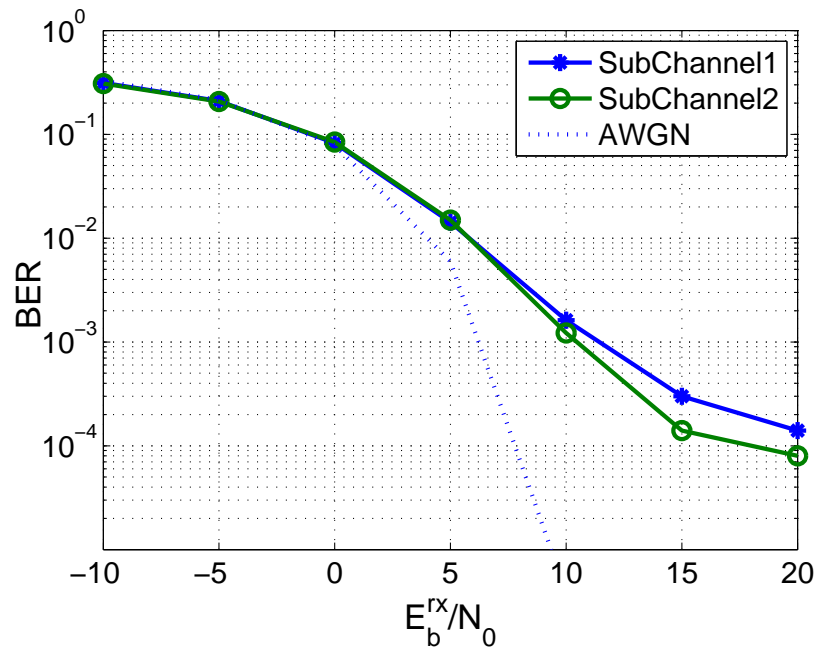


Fig. 11. BER performance for a 2×2 TR-MIMO system. ISI, IPI, and inter channel interference have been considered.